Botanical Sciences 103 (Special Issue): S23-S37. 2025
DOI: 10.17129/botsci.3667

Received: February 5, 2025, Accepted: April 19, 2025
On line first: July 31, 2025

Genetics / Genética

The complete mitochondrial genome of the hemiparasitic mistletoe *Psittacanthus palmeri* (Loranthaceae) and comparative analysis of mitogenomes across Santalales

Saddan Morales-Saldaña and Juan Francisco Ornelas*

Departamento de Biología Evolutiva, Instituto de Ecología, A.C., Xalapa, Veracruz, Mexico.
*Author for correspondence: francisco.ornelas@inecol.mx

Abstract

Background: In parasitic plants, it remains uncertain whether size, structure, and mutation rates in the mitogenome aligns with those of other angiosperms, and whether reduction in gene content is found across lineages of parasitic plants.
Question: Are there differences in gene loss patterns and selective pressures among mistletoe species in the order Santalales?
Studied species: *Psittacanthus palmeri* (Loranthaceae).
Study site: Santa María Tecomavaca, Oaxaca.
Methods: We assembled and annotated the mitogenome of *P. palmeri*. Then, we characterized the gene content, number and type of repeat sequences, and identified the mitochondrial plastid sequences. Finally, we reconstructed a phylogenetic tree for analysis of synteny and estimation of Ka/Ks ratios.
Results: The circular *P. palmeri* mitogenome (232,342 bp) contains 55 unique genes. Repeat analysis identified 52 microsatellites and 15 tandem repeats, along with 60 plastid sequences (43,874 bp, 18.9 %). Phylogenetic comparison revealed limited synteny (<7 kb), suggesting frequent rearrangements. Ka/Ks analysis indicated negative selection in *atp1*, *atp8*, *cob*, *cox1*, *nad9*, *rpl5*, and *rps12*, and positive in *ccmB*, *cox3*, *matR*, *mttB*, *nad3*, *nad4*, *nad4L*, *nad7*, *rps4*, and *rps10*.
Conclusions: The *P. palmeri* mitogenome is similar to those of other Santalales species in gene content, but differs in content of repeat sequences, and type and length of mitochondrial plastid sequences. Incorporating these features in future studies will allow to make inferences about expansion/contraction patterns that the mitogenomes have experienced during Santalales evolution.
Keywords: Ka/Ks, Mitochondrial plastid sequences, Parasitic plants.

Resumen

Antecedentes: En plantas parásitas, sigue siendo incierto si el tamaño, la estructura y las tasas mutacionales del mitogenoma se alinean con los de otras angiospermas, y si se reduce el contenido genético en otros linajes de plantas parásitas.
Pregunta: ¿Existen diferencias en los patrones de pérdida de genes y las presiones selectivas entre especies de muérdago del orden Santalales?
Especie estudiada: *Psittacanthus palmeri* (Loranthaceae).
Sitio de estudio: Santa María Tecomavaca, Oaxaca.
Métodos: Ensamblamos y anotamos el mitogenoma de *P. palmeri*. Luego, caracterizamos el contenido genético, número y tipo de secuencias repetidas, e identificamos las secuencias de plástidos mitocondriales. Finalmente, reconstruimos un árbol filogenético analizando la sintenia y estimamos las proporciones Ka/Ks.
Resultados: El mitogenoma circular de *P. palmeri* (232,342 pb) contiene 55 genes únicos. El análisis repetido identificó 52 microsatélites y 15 repeticiones en tándem, junto con 60 plástidos mitocondriales (43,874 pb, 18.9 %). La comparación filogenética reveló una sintenia limitada (<7 kb), sugiriendo reordenamientos frecuentes. El análisis Ka/Ks indicó selección negativa en *atp1*, *atp8*, *cob*, *cox1*, *nad9*, *rpl5* y *rps12*, y positiva en *ccmB*, *cox3*, *matR*, *mttB*, *nad3*, *nad4*, *nad4L*, *nad7*, *rps4*, y *rps10*.
Conclusiones: El mitogenoma de *P. palmeri* es similar a los de otras especies de Santalales en contenido genético, pero difiere en contenido de las secuencias repetidas, y en el tipo y longitud de las secuencias de plástidos mitocondriales. La incorporación de estas características en futuros estudios permitirá hacer inferencias acerca de los patrones de expansión/contracción que han experimentado los mitogenomas durante la evolución de Santalales.
Palabras clave: Ka/Ks, Secuencias del plástido mitocondrial, Plantas parásitas.

Parasitic plants range along a continuum from obligatory photosynthetic plants (root and stem parasites like mistletoes) or facultative photosynthetic (euphytoid parasites) to non-photosynthetic plants (root holoparasites and endophytic parasites). The evolutionary trajectories along the continuum of parasitism, from autotrophism towards hemiparasitism or holoparasitism, seem to be correlated with the loss of key photosynthesis and housekeeping genes in the plastome (Molina *et al*. 2014, Wicke *et al*. 2016). Sequencing of the plastomes of numerous parasitic angiosperms has found pronounced variation in size, structure, and gene content, suggesting a clear differentiation between plastomes of holoparasites, which have either functionally or completely lost most, or all genes involved in photosynthesis, and plastomes of hemiparasitic plants capable of photosynthesis (Wolfe *et al*. 1992, Petersen *et al*. 2015, Schneider *et al*. 2018, Banerjee & Stefanović 2020). However, mitochondrial evolution has comparatively received less attention.

Mitochondria, through oxidative phosphorylation, are essential producers of cellular energy, harboring key metabolic genes that control respiration, stress responses, and additional defense against microorganisms and aspects of programmed cell apoptosis (McBride *et al*. 2006, Friedman & Nunnari 2014, Gualberto *et al.* 2014). The embryophytes' mitochondrial genomes (hereafter mitogenome) are remarkably divergent in terms of size, structure, mutation rates, and RNA editing (Knoop 2012, Sloan *et al*. 2012, Yurina & Odintsova 2016, Gualberto & Newton 2017, Kozik *et al*. 2019, Petersen *et al*. 2020). Mitogenome size ranges from ca. 200 kb to 700 kb, although in *Silene conica* Geners. ex Rohrb. (Caryophyllaceae) the size is 11.3 Mb, 10 to almost 1,000 times larger than their animal counterparts (Sloan *et al*. 2012). The mitogenome size variation has been partly attributed to noncoding sequences that are not conserved across species, repeat sequences, and stretches of DNA transferred either from the nuclear and chloroplast genomes or from bacteria and viruses that have infected the plant (Alverson *et al*. 2011, Sloan *et al*. 2012, Gualberto & Newton 2017). The inclusion of foreign DNA, known as horizontal gene transfer (HGT), is relatively common in mitogenomes of angiosperms (Mower *et al*. 2004, 2010, Kozik *et al*. 2019, Petersen *et al*. 2020), and especially common in parasitic plants. In these plants, HGT is facilitated by the intimate connection between parasites and their host plant through haustoria, and genes are likely acquired via a single, DNA-mediated transfer event (Mower *et al*. 2010). However, the mechanisms, extent, and consequences of HGT remain largely unknown (Barkman *et al*. 2007, Westwood *et al*. 2010).

The structure of plant mitogenomes can be circular, linear, or branched, comprising one or more molecules (Notsu *et al*. 2002, Handa 2003, Sloan *et al*. 2012). The gene content of plant mitogenomes is largely conserved, containing all the genes present in the animal mitogenomes, with additional subunits in respiratory complex I: *nad7*, *nad9*, V: *atp1*, *atp4*, *atp9*, as well as in complex II: *sdh3*, *sdh4* (Zervas *et al*. 2019). In addition to the genes of the respiratory chain, plant mitogenomes contain a maturase-related protein gene (*matR*), genes encoding for proteins of the small and large subunit of the ribosomes (*rps* and *rpl* genes), and the genes *ccmB*, *ccmC*, *ccmFc*, and *ccmFn* that are involved in the cytochrome *c* biogenesis pathway. All genes from complexes I, III, IV, and V, which are considered as the core mitochondrial genes, are present in most sequenced autotrophic land plants (Adams & Palmer 2003, Petersen *et al*. 2015, Skippington *et al*. 2015), whereas the remaining genes comprise a variable part of the plant mitogenome (Zervas *et al*. 2019). Hence, the evolution of mitogenomes, which are involved in basic cell metabolism, is not expected to be influenced by the occurrence of parasitism though largely unexplored (Zervas *et al*. 2019, Petersen *et al*. 2020). Previous studies indicate that the gene content of the mitogenomes of parasitic plants is similar to patterns described above for other known angiosperm mitogenomes (Molina *et al*. 2014, Bellot *et al*. 2016). However, recent studies on four species of *Viscum* L. and one *Phoradendron* Nutt. species (Viscaceae) have shown a surprising reduction in gene content compared to all other known angiosperm mitogenomes (Petersen *et al*. 2015, Skippington *et al*. 2015, Darshetkar *et al*. 2023). This prompts the question as to whether gene loss in the mitogenome observed in *Viscum* and *Phoradendron* is found in other parasitic lineages as well. In addition to extensive gene loss, a very high level of sequence divergence and very high substitution rates have also been observed in the four species of *Viscum* and the one of *Phoradendron* as compared as to other plants (Bromham *et al*. 2013, Petersen *et al*. 2015, Skippington *et al*. 2015, Zervas *et al*. 2019), especially the genes in respiratory complex V, *atp1*, *apt6*, *atp8*, and *atp9*. In this context, Santalales offers an important model for studying the evolution of plant

parasitism due to harboring the widest array of nutritional modes and functional groups (Nickrent 2020, Teixeira-Costa & Davis 2021).

Psittacanthus Mart. (Loranthaceae) is the most species-rich genus of hemiparasitic mistletoes in the Psittacantheae tribe (ca. 110 species; Kuijt 2009, Dettke & Caires 2021), parasitizing a large host species range. *Psittacanthus palmeri* (S. Watson) Barlow & Wiens is a leaf deciduous hemiparasite only growing on *Bursera* Jacq. Ex L. species (Kuijt 2009, Ortiz-Rodriguez *et al*. 2018, Queijeiro-Bolaños *et al*. 2025). It is widely distributed in the seasonally dry tropical deciduous forest (hereafter SDTDF) in western and central regions of Mexico west of the Isthmus of Tehuantepec, in the central valleys of Oaxaca, and in the Central Depression of Chiapas near the border with Guatemala (Kuijt 2009, Ortiz-Rodriguez *et al*. 2018). Although *P. palmeri* primarily inhabits SDTDFs, it is also found in transitional zones between xeric scrub and pine-oak forests across its distribution range, which spans elevations from 400 to 2,150 m above sea level (Kuijt 2009).

While the chloroplast genome of *P. palmeri* has been assembled and compared with other five species of *Psittacanthus* (Morales-Saldaña *et al*. 2025), no mitogenomes have been sequenced yet. This study aims to (1) assemble and characterize the first mitogenome for *Psittacanthus* using Illumina sequencing reads, and (2) to compare that mitogenome with its plastome and with mitogenomes in other Santalales using a phylogenetic approach. This study represents the initial step in the *Psittacanthus* mitochondrial genome research, enriching genome resources for parasitic plants.

Material and methods

Sampling. We collected and preserved in silica gel young leaves from individual plants of *Psittacanthus palmeri* (*C. Soberanes CPC139*, XAL) at Cañón del Sabino, Santa María Tecomavaca, Oaxaca (17° 51’ 53” N, 97° 02’ 10” W, 725 m asl).

DNA extraction and sequencing. Total genomic DNA was extracted using a Dneasy Plant Mini kit (Qiagen, Valencia, CA, USA) using the manufacturer’s protocol and used for library preparation. DNA quality was measured using a NanoDrop spectrophotometer 2000 (ThermoFisher Scientific, Waltham, MA, USA) and 1 % agarose gels, and DNA quantity was analyzed with Qubit v. 2.0 (Life Technologies, Carlsbad, CA, USA). Paired-End (PE) sequencing using the Illumina Hi-Seq PE100 platform (San Diego, CA, USA) yielded approximately 254 G of raw reads. Raw Illumina reads were filtered using Trimmomatic v. 0.38 (Bolger *et al*. 2014) with the following parameters: SLIDING WINDOW:4:20 LEADING:5 TRAILING:0 MINLEN:75.

Mitogenome assembly and annotation. GetOrganelle v. 1.7.5 (Jin *et al*. 2020) was used to build contigs with the parameters R 30 -k 15,21,35,45,55,65,75,85,105,115,125 -w 65 -F embplant_mt. These contigs were mapped by BWA v. 0.7.17 (Li & Durbin 2009) to the mitogenome of *Santalum album* L. (Santalaceae), which was used as a reference to generate a seed sequence. Then, Illumina-filtered reads were mapped iteratively by BWA v. 0.7.17 (Li & Durbin 2009) to expand the sequence, ultimately revealing its primary structure. Finally, the assembled mitogenome was aligned with the Illumina filtered reads and improved through Pilon v. 1.22 (Walker *et al*. 2014) by 10 iterations to correct errors.

To annotate the mitogenome, we employed GeSeq (Tillich *et al*. 2017) and Intelligent Plant Mitochondrial Genome Annotator (IPMGA, https://www.1kmpg.cn/pmga/, Li *et al*. 2024, Zhang *et al*. 2024). The tRNAs were identified using tRNAscan-SE v. 2.0.7 with default parameters (Chan & Lowe 2019). We used Geneious Prime 2025.0.2 (Kearse *et al*. 2012) to manually verify the start and end codons and the annotations were double checked. Finally, the mitogenome graphic representation was made with the OGDRAW tool (https://chlorobox.mpimp-golm.mpg.de/OGDraw.html, Greiner *et al*. 2019). The complete mitogenome sequences assembled in this study were deposited into the GenBank database under the PQ723355 accession number.

Analysis of repeat sequences. We analyzed the presence of repeat sequences in three categories: simple sequence repeats (SSRs), tandem repeats, and dispersed repeats. SSRs were identified using the MISA web tool (https://web-blast.ipk-gatersleben.de/misa/, Beier *et al*. 2017) using the following parameters: the minimum number of repeats

for mononucleotides, dinucleotides, trinucleotides, tetranucleotides, pentanucleotides, and hexanucleotides were set to 10, 5, 4, 3, 3 and 3, respectively. The minimum threshold in a compound SSRs was set to be 100 bp. We identified tandem repeats using the Tandem Repeats Finder (TRF, https://tandem.bu.edu/trf/trf.html, Benson 1999) with the default parameters. Lastly, dispersed repeats including forward repeat sequences, reverse repeat sequences, palindromic repeat sequences, and complementary repeat sequences were identified by REPuter (https://bibiserv.cebitec.uni-bielefeld.de/reputer, Kurtz *et al*. 2001), setting the Hamming distance of 3, a minimum repeat size of 30 bp, and a maximum of 5,000 computed repeats.

Identification of the mitochondrial plastid sequences (MTPTs). We used the chloroplast genome of *P. palmeri* (PP236144) assembled by Morales-Saldaña *et al*. (2025) to contrast it with its mitogenome and to identify the mitochondrial plastid sequences (MTPTs). We used the BLASTn tool (Chen *et al*. 2015) with the e-value cutoff set as 1*e*-5, and a minimum match of 100 bp. The MTPTs with matching rates ≥ 80 % and lengths ≥ 40 bp were selected. All the results were manually annotated to verify the presence of genes within the MTPTs.

Phylogenetic tree building and comparative analyses in Santalales mitogenomes. To understand the evolutionary dynamics of *P. palmeri* mitogenome in a comparative context, we constructed a phylogenetic tree with seven mitogenomes of other Santalales retrieved from the National Center for Biotechnology Information (NCBI) database. These included *Helicanthes elastica* (Desr.) Danser (NC072104) and *Tolypanthus maclurei* Danser (NC056836) in Loranthaceae, *Malania oleifera* Chun & S.K.Lee (NC053625) in Olacaceae, *Santalum album* L. (NC081498) in Santalaceae, and *Viscum album* L. (KJ29610), *Viscum diospyrosicola* Hayata (PQ046266) and *Viscum scurruloideum* Barlow (KT022222, KT022223) in Viscaceae. Because of the ambiguous position of Santalales within eudicotyledons, no outgroups outside of Santalales were used (Nickrent *et al*. 2019). The conserved Protein Coding Genes (PCGs) from all species were extracted by PhyloSuit v. 1.2.3 software (Zhang *et al*. 2020) and aligned with MAFFT v. 7.505 software (Katoh *et al*. 2019). The phylogenetic analysis was performed employing concatenated sequences from seven PCGs using a maximum-likelihood (ML) approach in RAxML v. 8.2.10 (Stamatakis 2014) with 1,000 rapid bootstrap replicates using the best-fit nucleotide substitution model (GTR-GAMMA+I) estimated from ModelTest-NG v. 0.17 (Darriba *et al*. 2020) by the AIC, BIC and AICc methods.

The phylogenetic tree obtained was used as an evolutionary framework to analyze the *P. palmeri* mitogenome against other Santalales species. We visualized the conservation of gene order among Santalales mitogenomes, generating a synteny plot with the pyGenomeViz v. 0.2.1 package, employing the pgv-mmseqs mode and setting an identity threshold of 50 % (https://github.com/moshi4/pyGenomeViz). Also, we conducted pairwise comparisons to estimate the frequencies of synonymous (Ks) and non-synonymous (Ka) substitutions across 32 PCGs to assess potential selective pressures during evolutionary dynamics. Under neutral selection, Ks equals Ka, resulting in a Ka/Ks ratio of 1. A Ka/Ks ratio greater than 1 (Ka > Ks) suggests positive selection, whereas a ratio less than 1 (Ks > Ka) indicates negative selection. Because there are no available mitogenomes of autotrophic Santalales species, we used *Malania oleifera* mitogenome as a reference to evaluate the dynamics in the Ka/Ks ratio changes between root-hemiparasitic species and stem-hemiparasitic species (mistletoes). Thirty-two PCGs were aligned individually using MAFFT v. 7.505 software (Katoh *et al*. 2019), and then Ks/Ka ratios were calculated with Ka/Ks calculator v. 2.0 using the MLWL model (https://sourceforge.net/projects/kakscalculator2/, Wang *et al*. 2010). The *rpl16* gene was excluded from the analysis due to its plastid origin.

Results

Mitogenome structure and gene content. Using Illumina sequencing data, we assembled a circular mitogenome of 232,342 bp for *P. palmeri* (Figure 1A). The total guanine and cytosine (GC) content was 44.8 %. We identified 73 mitochondrial genes (55 unique genes), including 36 PCGs (33 unique), from which 26 genes (21 unique) correspond to core genes and 10 are variable genes (Table 1). PCGs include nine cis-splicing genes (*ccmFc*, *cox2*, *nad2*, *nad4*, *nad7*, *rps10*, *trnA-UGC* (×2), and *trnL-UAA*), two trans-splicing genes (*nad1* and *nad5*) (Figures S1-S2), and one

derived-plastome gene (*rpl116*). Two copies of *atp9* and *nad4L* genes were annotated, but we could not determine the start codon for three genes (*cox1*, *cox3*, *rps10*). The total length of all 36 PCGs was 28,407 bp, representing 12.2 % of the *P. palmeri* mitogenome (Figure 1B).

The mitogenome of *P. palmeri* also comprises 32 tRNA genes (19 unique). Out of these, 10 are native to the mitochondria, whereas others such as *trnA-UGC*, *trnfM-CAU*, *trnI-CAU*, *trnD-GUC*, *trnN-GUU*, *trnR-ACG*, *trnH-GUC*, *trnS-GGA*, *trnT-UGU*, *trnL-UAA*, *trnF-GAA*, and *trnW-CCA*, are derived from plastids. Also, we identified two copies of *rrn5* and *rrn26* genes and one single copy of *rrn18* gene. The collective lengths of tRNA and rRNA genes constitute 1 % (2,429 bp) and 3 % (6,965 bp), respectively. Finally, three conserved gene clusters are present in the mitogenome, namely *cox3-sdh4*, *18S-5S* rRNAs, and *nad3-rps12*. The non-coding regions represent 83.7 % of the total length of the mitogenome (Figure 1B).

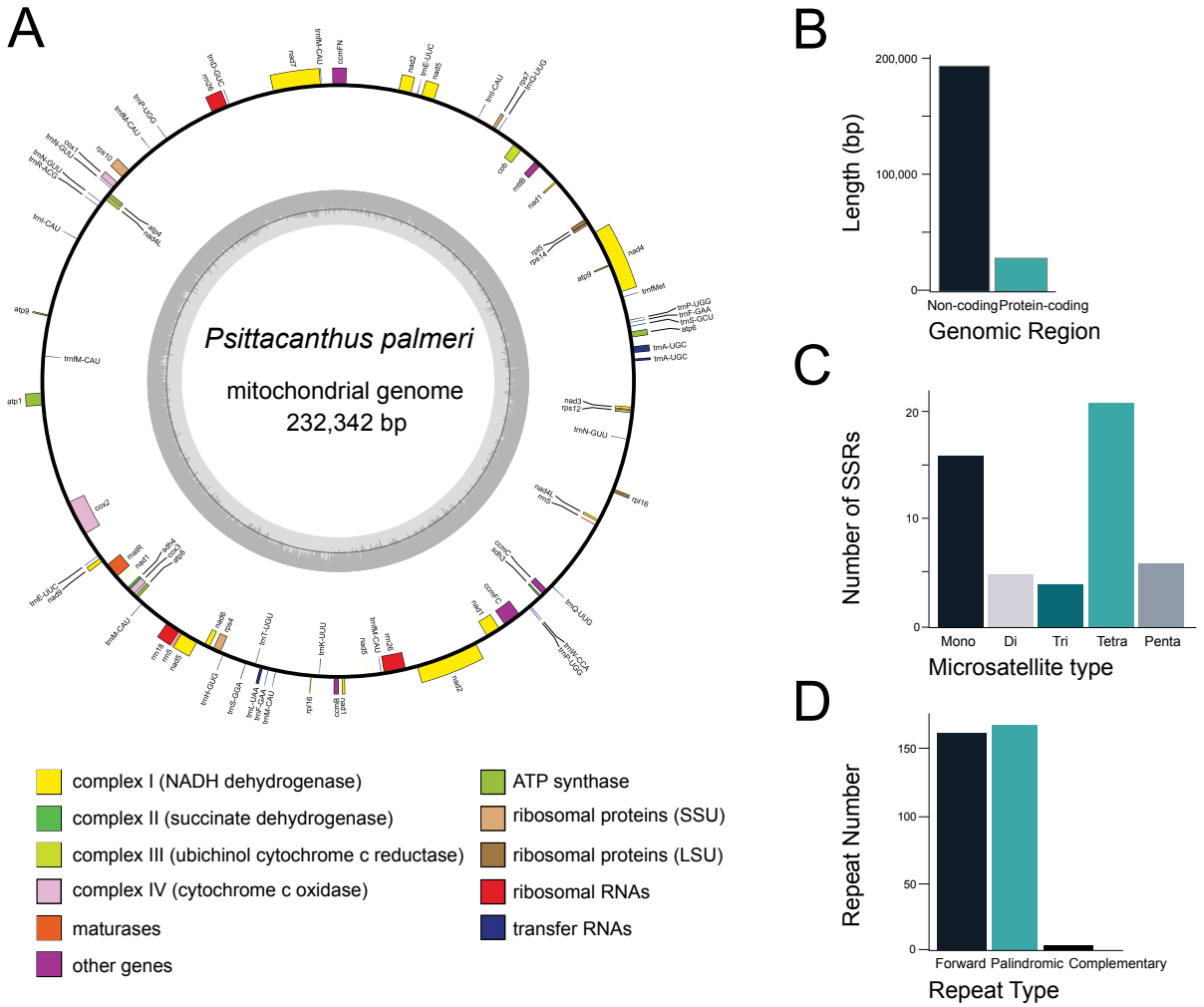

Figure 1. A) Genomic map of the *Psittacanthus palmeri* mitogenome. Genes shown on the outside of the map are transcribed clockwise, whereas genes on the inside are transcribed counter-clockwise. Genes are color coded by their function in the legend. B) Proportion of coding and non-coding regions in the *P. palmeri* mitogenome. C) Microsatellites detected. Mono, Di, Tri, Tetra, and Penta represent mononucleotide, dinucleotide, trinucleotide, tetra-nucleotide, and pentanucleotide, repeats, respectively. D) Predicted repeats (forward, palindromic, complementary) in the *P. palmeri* mitogenome.

Table 1. Gene content of the *Psittacanthus palmeri* mitogenome.

Group of genes	Name of genes
Complex I (NAD dehydrogenase)	*nad1*, *nad2*, *nad3*, *nad4*, *nad4L* (×2), *nad5*, *nad6*, *nad7*, *nad9*
Complex II (ubiquinol cytochrome c reductase)	*cob*
Complex IV (cytochrome c oxidase)	*cox1*, *cox2*, *cox3*
Complex V (ATP synthase)	*atp1*, *atp4*, *atp6*, *atp8*, *atp9* (×2)
Cytochrome c biogenesis	*ccmB*, *ccmC*, *ccmFC*, *ccmFN*
Large subunit of ribosomal proteins (LSU)	*rpl5*, *rpl16* (×2)
Small subunit of ribosomal proteins (SSU)	*rps4*, *rps7*, *rps10*, *rps12*, *rps14*
Intron maturase	*matR*
Transport membrane protein	*mttB*
Succinate dehydrogenase genes	*sdh3*, *sdh4*
Ribosomal RNA	*rrn5* (×2), *rrn18*, *rrn26* (×2)
Transfer RNA	*trnA-UGC* (×2), *trnD-GUC*, *trnE-UUC* (×2), *trnF-GAA* (×2), *trnfM*-CAU (×4), *trnfMet*, *trnH*-GUG, *trnI*-CAU (×2), *trnK*-UUU, *trnL*-UAA, *trnM*-CAU (×2), *trnN*-GUU (×3), *trnP*-UGG (×3), *trnQ*-UUG (×2), *trnR*-ACG, *trnS*-GCU, *trnS*-GGA, *trnT*-UGU, *trnW*-CCA

Repeat sequence analysis and identification of mitochondrial plastid sequences. A total of 52 SSRs were identified in the *P. palmeri* mitogenome, including 16 monomers (30.8 %), 5 dimers (9.6 %), 4 trimers (7.7 %), 21 tetramers (40.4 %), and 6 pentamers (11.5 %). Hexamers were not detected (Figure 1C). For the monomers, 13 A/T sequences (81.2 %) occupied the main proportion, while G/C represented only 18.8 % (3 sequences), whereas the dinucleotide AT/AT repeat unit showed the highest frequency. The trinucleotide AAT/ATT and tetranucleotide AAAG/CTTT repeat units were the most common. Tetramers showed the highest frequency among the various repeat types of SSRs identified within the *P. palmeri* mitogenome (Figure 1C). Further, we identified 15 tandem repeats with consensus sizes ranging from 22 to 452 bp. These repeats had a sequence similarity of over 74 %. Additionally, we identified 413 pairs of dispersed repeats that were 30 bp or longer, from which 217 pairs were palindromic, 195 pairs were forward repeats, and one pair was complementary. No reverse repeats were detected. The length of the dispersed repeat sequences ranged from 30 to 1,528 bp (Figure 1D). The longest forward repeat was 641 bp, the longest palindromic repeat was 1,528 bp, and the complementary repeat was 30 bp in length. These dispersed repeats represented 38.1 % of the *P. palmeri* mitogenome.

The comparison between the mitogenome and the plastome of *P. palmeri* yielded 60 highly-similar regions (> 80 %) (Figure 2). These 60 fragments have a length of 43,874 bp, representing 18.9 % of the mitogenome. The longest fragment was 5,061 bp, and the shortest was only 40 bp. We annotated these MTPTs and identified 16 tRNA genes (*trnA-UGC* (×2), *trnD-GUC*, *trnI-CAU* (×3), *trnF-GAA*, *trnH-GUC*, *trnL-UAA*, *trnM-CAU*, *trnN-GUU* (×3), *trnR-ACG*, *trnS-GGA*, *trnT-UGU*), and one single protein-coding gene (*rpl16*) (Figure 2).

Phylogenetic tree and comparative analyses of Santalales mitogenomes. The final alignment of seven PCGs shared by all species was 8,646 bp and 18.49 % of missing data. All nodes of the phylogenetic tree had bootstrap support (BS) values > 95 (Figure S3). The synteny plot showed short stretches (less than 7 kb) of synteny across all species (Figure 3). In addition, there were many sequence rearrangements, and the order of the mitogenome was not conserved despite their phylogenetic relationships (Figure 3).

We found divergent patterns for the Ka/Ks ratios according to gene classes and lineages analyzed (Figure 4). According to pairwise comparisons, the genes *atp1*, *atp8*, *atp9*, *ccmC*, *cob* (except *S. album*), *cox1*, *nad9*, and *rps12*

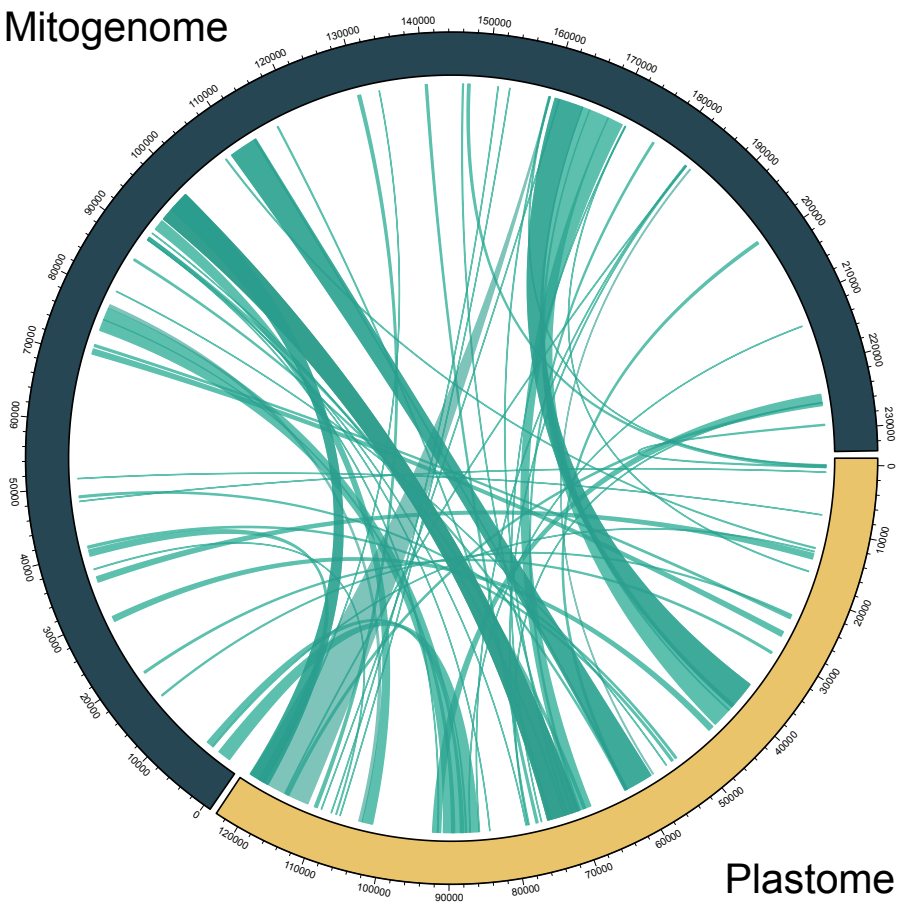

Figure 2. Sequences transfer from the chloroplast to the mitochondrial genome in *Psittacanthus palmeri*. The ribbon width is proportional to the sequence length.

showed low (< 1) and significant ($P < 0.05$) Ka/Ks ratios in most comparisons, indicating negative possibly purifying selection. In contrast, *ccmB*, *matR*, *nad3*, *nad4*, and *rps10* genes showed high Ka/Ks values (> 1) in most comparisons, suggesting potential positive selection, but pairwise comparisons were not statistically significant ($P > 0.05$).

We also identified lineage-specific patterns. For example, all genes in the *Viscum* mitogenomes showed low and significant Ka/Ks values, except *ccmB* and *matR* genes in *V. album* (> 1, $P > 0.05$), and *rps10* in *V. scurruloideum* (0.76, $P > 0.05$). The highest Ka/Ks values were found in the *rps7* gene for *H. elastica* and *T. maclurei* (Loranthaceae) and *mttB* for *S. album* (Santalaceae). Finally, the *P. palmeri* mitogenome showed potential purifying selection for *atp1*, *atp8*, *cob*, *cox1*, *nad9*, *rpl5*, and *rps12* (Ka/Ks < 1, $P < 0.05$), while the highest non-significant Ka/Ks values were identified in *ccmB*, *cox3*, *matR*, *mttB*, *nad3*, *nad4*, *nad4L*, and *rps4* genes (Figure 4).

Discussion

The limited number of complete mitogenome sequences of the autotrophic and hemiparasitic species within Santalales order (only seven to date) has revealed the presence of all 24-core protein-coding genes, except *nad1*, *nad4*, and *cox2* genes, which were found to be pseudogenized in *Helicanthes elastica* (Darshetkar *et al*. 2023) or lost in the mitogenomes of *Phoradendron ligra* and *Viscum* species (Petersen *et al*. 2015, Skippington *et al*. 2015, 2017, Zervas *et al*. 2019). In this study, we assembled and characterized the complete mitogenome of *Psittacanthus palmeri*, the first for a New World Loranthaceae, establishing an important precedent in the survey of mitogenome evolution for one of the most diverse genera of mistletoes.

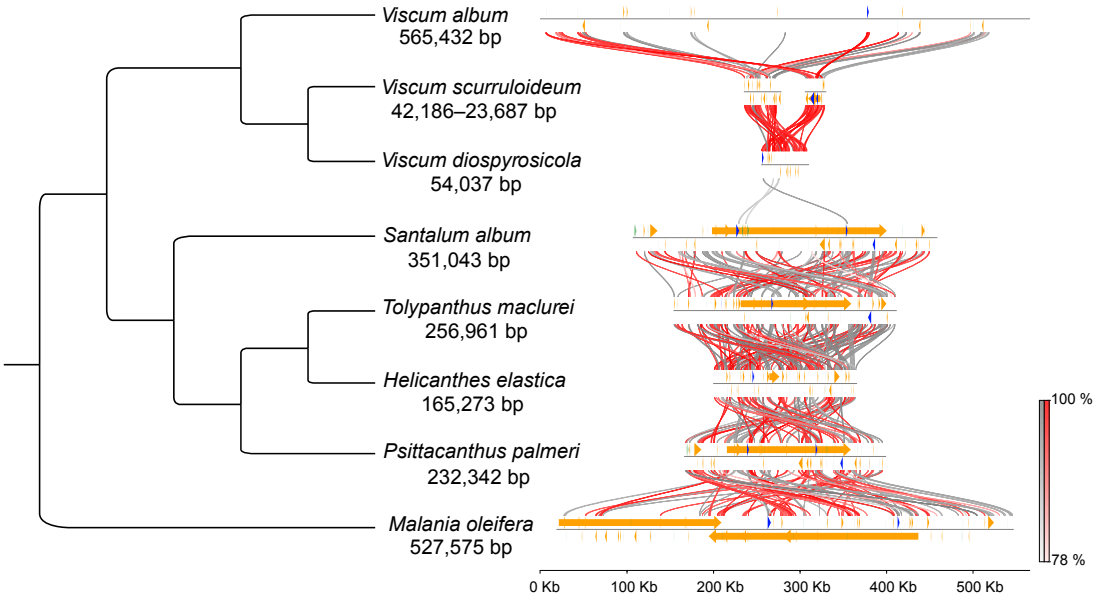

Figure 3. Collinearity analysis (synteny plot) of the mitogenomes of eight Santalales species displayed according to phylogenetic tree based on Maximum Likelihood. All nodes had bootstrap support values > 95 (Figure S3). The synteny plot shows short stretches (less than 7 kb) of synteny across all species and non-conserved mitogenomes despite their phylogenetic relationships.

Similar gene content but abundant repeats in Psittacanthus palmeri. Angiosperms mitogenome sequenced until now have shown remarkable variation in the size (Sloan *et al*. 2012, Skippington *et al*. 2015), occurring even within a single family or genus (Alverson *et al*. 2010, Petersen *et al*. 2015, Skippington *et al*. 2015, 2017). Interestingly, nearly all angiosperm mitogenomes assembled so far have core genes, showing only variation in the presence of genes encoding ribosomal proteins (*rps* and *rpl*) and succinate dehydrogenase subunits (*sdh*), which are particularly prone to be lost (Zervas *et al*. 2019, Mower 2020). Adams *et al*. (2001) reported that some of these genes, particularly *sdh*, have been transferred to the nucleus during recent angiosperm evolution. The size of the *P. palmeri* mitogenome of 232,342 bp and the 44.8 % GC content are consistent values reported for other angiosperms including Loranthaceae members (Yu *et al*. 2021, Darshetkar *et al*. 2023), but unlike other confamilial species (*e.g*., *Helicanthes elastica*, *Tolypanthus maclurei*), the *P. palmeri* mitogenome did not show pseudogenized genes. Furthermore, consistent with other hemiparasitic Santalales, all core protein-coding genes were annotated, whereas several ribosomal protein genes, including large (*rpl2*, *rpl10*) and small (*rps1*, *rps2*, *rps3*, *rps11*, *rps13*, and *rps19*) subunit genes, were absent (Zervas *et al*. 2019). Even species that exhibit substantial gene loss (*e.g.*, *Phoradendron liga* and *Viscum* spp.) also have shown a remarkable mitogenome size variation (Petersen *et al*. 2015, Skippington *et al.* 2015, 2017, Zervas *et al*. 2019), suggesting that size differences observed in Santalales mitogenome do not appear to reflect major differences in gene content.

Complementary hypotheses to gene content variation have been proposed to explain the maintenance and evolution of mitogenome size. These include the presence of transposable and repetitive elements (Bennetzen 2005, Wynn & Christensen 2019), as well as the inter-organelle DNA transfer (Alverson *et al*. 2010, Sloan & Wu 2014, Gandini & Sanchez-Puerta 2017). However, repetitive elements and mitochondrial plastid sequences remain poorly characterized in the Santalales (Skippington *et al.* 2015, Liu *et al*. 2024). Repetitive sequences cover ≈ 90 kb (39 %) of the *P. palmeri* mitogenome, which is notably greater than the ≈ 19 kb (5.41 %) reported for *S. album* (Liu *et al*. 2024), and the 26 kb, although similar in proportion (39 %), reported for *V. scurruloideum* mitogenome (Skippington *et al*. 2015). In contrast to the high synteny levels observed among Santalales species plastomes (Tang *et al*. 2024, Morales-Saldaña *et al*. 2025), the high rearrangement rates observed among Santalales mitogenomes could be explained by doubled-strand break repair hypothesis, as a generator mechanism of repeated sequences associated with recombinationally active sites causing constant rearrangements (Sloan 2013, Wynn & Christensen 2019).

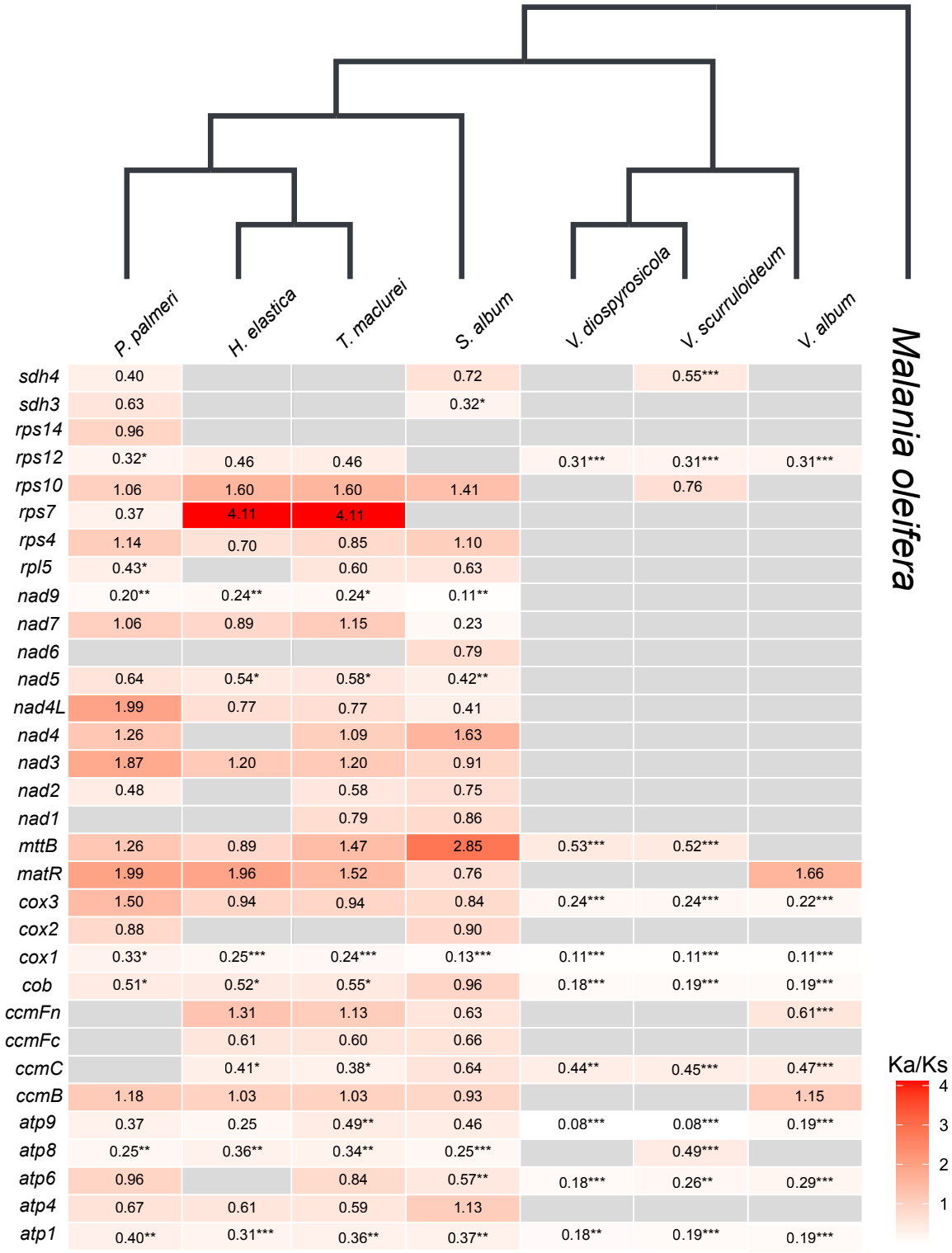

	P. palmeri	H. elastica	T. maclurei	S. album	V. diospyrosicola	V. scurruloideum	V. album
sdh4	0.40			0.72		0.55***	
sdh3	0.63			0.32*			
rps14	0.96						
rps12	0.32*	0.46	0.46		0.31***	0.31***	0.31***
rps10	1.06	1.60	1.60	1.41		0.76	
rps7	0.37	4.11	4.11				
rps4	1.14	0.70	0.85	1.10			
rpl5	0.43*		0.60	0.63			
nad9	0.20**	0.24**	0.24*	0.11**			
nad7	1.06	0.89	1.15	0.23			
nad6				0.79			
nad5	0.64	0.54*	0.58*	0.42**			
nad4L	1.99	0.77	0.77	0.41			
nad4	1.26		1.09	1.63			
nad3	1.87	1.20	1.20	0.91			
nad2	0.48		0.58	0.75			
nad1			0.79	0.86			
mttB	1.26	0.89	1.47	2.85	0.53***	0.52***	
matR	1.99	1.96	1.52	0.76			1.66
cox3	1.50	0.94	0.94	0.84	0.24***	0.24***	0.22***
cox2	0.88			0.90			
cox1	0.33*	0.25***	0.24***	0.13***	0.11***	0.11***	0.11***
cob	0.51*	0.52*	0.55*	0.96	0.18***	0.19***	0.19***
ccmFn		1.31	1.13	0.63			0.61***
ccmFc		0.61	0.60	0.66			
ccmC		0.41*	0.38*	0.64	0.44**	0.45***	0.47***
ccmB	1.18	1.03	1.03	0.93			1.15
atp9	0.37	0.25	0.49**	0.46	0.08***	0.08***	0.19***
atp8	0.25**	0.36**	0.34**	0.25***		0.49***	
atp6	0.96		0.84	0.57**	0.18***	0.26**	0.29***
atp4	0.67	0.61	0.59	1.13			
atp1	0.40**	0.31***	0.36**	0.37**	0.18**	0.19***	0.19***

Figure 4. Pairwise Ka/Ks comparisons between frequencies of synonymous (Ks) and non-synonymous (Ka) substitutions for the 32 protein-coding genes (PCGs) in Santalales mitogenomes using *M. oleifera* mitogenome as a reference. Ks = Ka, under neutral selection (Ka/Ks = 1), Ka > Ks, under positive selection (Ka/Ks > 1), Ks > Ka under negative selection (Ka/Ks < 1). * = $P < 0.05$, ** = $P < 0.01$, *** = $P < 0.001$. Missing Ka/Ks values indicate cases where the ratio could not be calculated due to absent synonymous (Ks) or non-synonymous (Ka) substitutions in the compared gene pairs.

Mitochondrial plastid sequences (MTPTs) in Psittacanthus palmeri. Plastid-derived DNA in angiosperm mitogenomes has been widely documented across several lineages identifying a high diversity of patterns regarding the total length of MTPT sequences, the number of chloroplast genes included, and the percentage that MTPTs represent in the mitogenome (Wang *et al*. 2012, Nhat Nam *et al*. 2024). In the *P. palmeri* mitogenome, we identified 60 highly similar regions (> 80 %) with a total length of 43,874 bp representing ≈19 % of the mitogenome, a fraction remarkably higher than the 6.37 % reported for *S. album* mitogenome (Liu *et al*. 2024) and to 9.1 % reported for *T. maclurei* (Yu *et al*. 2021), being the highest proportion of chloroplast origin sequences reported until now for a species in the Santalales order. Also, 18 potentially functional plastid-derived genes were identified in these 60 MTPT sequences, indicating that approximately half of the tRNA genes have been transferred from the plastid. The function of both plastid-derived tRNA genes and non-coding sequences incorporated (if any) is unknown. Wang *et al*. (2012) suggested that incorporating novel mitochondrial genes could be an important source of genetic variation, unrelated to plastid functions, with potential implications for the mitogenome evolution in Santalales that need to be addressed in further studies.

Variation of mitochondrial genes among Santalales. Previous studies have found contrasting results regarding rates of molecular evolution in the mitochondrial genes of parasitic plants. Bromham *et al*. (2013) showed that parasitic plants have consistently faster rates of molecular evolution than their non-parasitic relatives in mitochondrial, chloroplast, and nuclear sequences. In contrast, Zervas *et al*. (2019) and Petersen *et al*. (2020) found no evidence that mitochondrial genes in parasitic plants evolve faster than their closest autotrophic relatives. In our study, we used Ka/Ks ratios to estimate the amino acid substitution rates among mitochondrial protein-coding genes in Santalales species and, as an indicator, to infer the direction and magnitude of potential selection pressures. Because there are no complete autotrophic species Santalales mitogenomes available, we contrasted the Ka/Ks ratios between mistletoes and *Malania oleifera*, the only root-hemiparasitic species with mitogenome available. Significantly low Ka/Ks ratios (negative selection) were observed in genes such as *nad9*, *cob*, *cox1*, *atp1*, and *atp8,* which participate in different oxidative phosphorylation stages (Zancani *et al*. 2020). These results suggest important functional restrictions in the generation of ATP through oxidative phosphorylation conducted by ATP synthase in *P. palmeri*. Conversely, we also detected genes with Ka/Ks ratios > 1 (*ccmB*, *cox3*, *matR*, *mttB*, *nad3*, *nad4*, *nad4L*, *nad7*, *rps4*, and *rps10*), which suggests potential positive or relaxed selection occurred in these genes during *P. palmeri* evolution. Nonetheless, results from pairwise comparisons using *M. oleifera* mitogenome as a reference to evaluate the dynamics in the Ka/Ks ratio changes were non-significant, which suggests the need for further testing to assess selective pressures on protein-coding genes.

Through the assembly and characterization of *Psittacanthus palmeri* mitogenome, we demonstrated that it is similar to those of other Santalales species concerning gene content, but different in the content of repeat sequences and the type and length of mitochondrial plastid sequences. Considering these features, rarely analyzed in Santalales, in conjunction with the availability of complete mitogenomes through several Santalales lineages, will allow us to make inferences regarding the expansion and contraction patterns that the mitogenomes have experienced during the evolution of Santalales. Also, Ka/Ks ratios observed in mitochondrial genes of *P. palmeri* highlight the need to continue evaluating mitogenome substitution rates, which will allow deeper insights into the adaptative value of these protein-coding genes. Based on these findings and the available sequences, we believe that our understanding of parasitic plant mitochondrial evolution is still limited, so increased lineage-sampling within the Santalales is a key step to understanding the molecular evolution of the mitogenome within parasitic plants.

Supplementary material

Supplemental data for this article can be accessed here: https://doi.org/10.17129/botsci.3667

Acknowledgements

The authors thank Carlos Soberanes, Yuyini Licona-Vera, Andrés E. Ortiz-Rodriguez, Etelvina Gándara, José Manuel García, and Eduardo Ruiz-Sanchez for help in the field, Antonio Acini Vásquez-Aguilar and Santiago Ramírez-Barahona for the help in the lab, and Emanuel Villafán and Enrique Ibarra-Laclette for the help in the HUITZIL cluster. The authors thank the UC Davis Genome Center DNA Core Facility (Research Resource Identifier: 01-38526438) for providing Illumina Hi-Seq PE100 sequencing facilities and services. Also, the authors thank Isaac Sandoval Padilla, one anonymous reviewer, and the associate editor for improving the quality of this manuscript.

Literature cited

Adams KL, Palmer JD. 2003. Evolution of mitochondrial gene content: gene loss and transfer to the nucleus. *Molecular Phylogenetics and Evolution* **29**: 380-95. https://doi.org/10.1016/S1055-7903(03)00194-5

Adams KL, Rosenblueth M, Qiu YL, Palmer JD. 2001. Multiple losses and transfers to the nucleus of two mitochondrial succinate dehydrogenase genes during angiosperm evolution. *Genetics* **158**: 1289-1300. https://doi.org/10.1093/genetics/158.3.1289

Alverson AJ, Wei X, Rice DW, Stern DB, Barry K, Palmer JD. 2010. Insights into the evolution of mitochondrial genome size from complete sequences of *Citrullus lanatus* and *Cucurbita pepo* (Cucurbitaceae). *Molecular Biology and Evolution* **27**: 1436-1448. https://doi.org/10.1093/molbev/msq029

Alverson AJ, Zhuo S, Rice DW, Sloan DB, Palmer JD. 2011. The mitochondrial genome of the legume *Vigna radiata* and the analysis of recombination across short mitochondrial repeats. *Plos One* **6**: e16404. https://doi.org/10.1371/journal.pone.0016404

Banerjee A, Stefanović S. 2020. Reconstructing plastome evolution across the phylogenetic backbone of the parasitic plant genus *Cuscuta* (Convolvulaceae). *Botanical Journal of the Linnean Society* **194**: 423-438. https://doi.org/10.1093/botlinnean/boaa056

Bennetzen JL. 2005. Transposable elements, gene creation and genome rearrangement in flowering plants. *Current Opinion in Genetics and Development* **15**: 621-627. https://doi.org/10.1016/j.gde.2005.09.010

Barkman TJ, McNeal JR, Lim S-H, Coat G, Croom HB, Young ND, dePamphilis CW. 2007. Mitochondrial DNA suggests at least 11 origins of parasitism in angiosperms and reveals genomic chimerism in parasitic plants. *BMC Evolutionary Biology* **7**: 248. https://doi.org/10.1186/1471-2148-7-248

Beier S, Thiel T, Münch T, Scholz U, Mascher M. 2017. MISA-web: a web server for microsatellite prediction. *Bioinformatics* **33**: 2583-2585. https://doi.org/10.1093/bioinformatics/btx198

Bellot S, Cusimano N, Luo S, Sun G, Zarre S, Gröger A, Temsch E, Renner SS. 2016. Assembled plastid and mitochondrial genomes, as well as nuclear genes, place the parasite family Cynomoriaceae in the Saxifragales. *Genome Biology and Evolution* **8**: 2214-2230. https://doi.org/10.1093/gbe/evw147

Benson G. 1999. Tandem repeats finder: a program to analyze DNA sequences. *Nucleic Acids Research* **27**: 573-580. https://doi.org/10.1093/nar/27.2.573

Bolger AM, Lohse M, Usadel B. 2014. Trimmomatic: a flexible trimmer for Illumina sequence data. *Bioinformatics* **30**: 2114-2120. https://doi.org/10.1093/bioinformatics/btu170

Bromham L, Cowman PF, Lanfear R. 2013. Parasitic plants have increased rates of molecular evolution across all three genomes. *BMC Evolutionary Biology* **13**: 1-11. https://doi.org/10.1186/1471-2148-13-126

Chan PP, Lowe TM. 2019. RNAscan-SE: Searching for tRNA Genes in Genomic Sequences. *In*: Kollmar, M. eds. *Gene Prediction. Methods in Molecular Biology*. New York, NY: Humana. pp. 1-14. https://doi.org/10.1007/978-1-4939-9173-0_1

Chen Y, Ye WC, Zhang YD, Xu YS. 2015. High speed BLASTN: an accelerated MegaBLAST search tool. *Nucleic Acids Research* **43**: 7762-7768. https://doi.org/10.1093/nar/gkv784

Darriba D, Posada D, Kozlov AM, Stamatakis A, Morel B, Flouri T. 2020. ModelTest-NG: a new and scalable tool for the selection of DNA and protein evolutionary models. *Molecular Biology and Evolution* **37**: 291-294. https://doi.org/10.1093/molbev/msz189

Darshetkar AM, Pable AA, Nadaf AB, Barvkar VT. 2023. Understanding parasitism in Loranthaceae: insights from plastome and mitogenome of *Helicanthes elastica*. *Gene* **861**: 147238. https://doi.org/10.1016/j.gene.2023.147238

Dettke GA, Caires CS. 2021. *Psittacanthus* (Loranthaceae) in Brazil: new occurrences, lectotypifications, new synonyms and an illustrated key. *Rodriguesia* **72**: e00602020. https://doi.org/10.1590/2175-7860202172138

Friedman JR, Nunnari J. 2014. Mitochondrial form and function. *Nature* **505**: 335-343. https://doi.org/10.1038/nature12985

Gandini CL, Sanchez-Puerta MV. 2017. Foreign plastid sequences in plant mitochondria are frequently acquired via mitochondrion-to-mitochondrion horizontal transfer. *Scientific Reports* **7**: 43402. https://doi.org/10.1038/srep43402

Greiner S, Lehwark P, Bock R. 2019. OrganellarGenomeDRAW (OGDRAW) version 1.3.1: expanded toolkit for the graphical visualization of organellar genomes. *Nucleic Acids Research* **47**: W59-W64. https://doi.org/10.1093/nar/gkz238

Gualberto JM, Newton KJ. 2017. Plant mitochondrial genomes: dynamics and mechanisms of mutation. *Annual Review of Plant Biology* **68**: 225-252. https://doi.org/10.1146/annurev-arplant-043015-112232

Gualberto JM, Mileshina D, Wallet C, Niazi AK, Weber-Lotfi F, Dietrich A. 2014. The plant mitochondrial genome: dynamics and maintenance. *Biochimie* **100**: 107-120. https://doi.org/10.1016/j.biochi.2013.09.016

Handa H. 2003. The complete nucleotide sequence and RNA editing content of the mitochondrial genome of rapeseed (*Brassica napus* L.): comparative analysis of the mitochondrial genomes of rapeseed and *Arabidopsis thaliana*. *Nucleic Acids Research* **31**: 5907-5916. https://doi.org/10.1093/nar/gkg795

Jin JJ, Yu WB, Yang JB, Song Y, DePamphilis CW, Yi TS, Li DZ. 2020. GetOrganelle: a fast and versatile toolkit for accurate de novo assembly of organelle genomes. *Genome Biology* **21**: 1-31. https://doi.org/10.1186/s13059-020-02154-5

Katoh K, Rozewicki, Yamada KD. 2019. MAFFT online service: multiple sequence alignment, interactive sequence choice and visualization. *Briefings in Bioinformatics* **20**: 1160-1166. https://doi.org/10.1093/bib/bbx108

Kearse M, Moir R, Wilson A, Stones-Havas S, Cheung M, Sturrock S, Buxton S, Cooper A, Markowitz S, Duran C, Thierer T, Ashton B, Meintjes P, Drummond A. 2012. Geneious Basic: an integrated and extendable desktop software platform for the organization and analysis of sequence data. *Bioinformatics* **28**: 1647-1649. https://doi.org/10.1093/bioinformatics/bts199

Knoop V. 2012. Seed Plant Mitochondrial Genomes: Complexity Evolving. In: Bock, R., Knoop, V. (Eds.), *Genomics of Chloroplasts and Mitochondria, Advances in Photosynthesis and Respiration*. Springer Netherlands, Dordrecht, pp. 175-200. https://doi.org/10.1007/978-94-007-2920-9_8

Kozik A, Rowan BA, Lavelle D, Berke L, Schranz ME, Michelmore RW, Christensen AC. 2019. The alternative reality of plant mitochondrial DNA: one ring does not rule them all. *Plos Genetics* **15**: e1008373. https://doi.org/10.1371/journal.pgen.1008373

Kuijt J. 2009. Monograph of *Psittacanthus* (Loranthaceae). *Systematic Botany Monographs* **86**: 1-362.

Kurtz S, Choudhuri JV, Ohlebusch E, Schleiermacher C, Stoye J, Giegerich R. 2001. REPuter: the manifold applications of repeat analysis on a genomic scale. *Nucleic Acids Research* **29**: 4633-4642. https://doi.org/10.1093/nar/29.22.4633

Li H, Durbin R. 2009. Fast and accurate short read alignment with Burrows-Wheeler transform. *Bioinformatics* **25**: 1754-1760. https://doi.org/10.1093/bioinformatics/btp324

Li J, Ni Y, Lu Q, Chen H, Liu C. 2024. PMGA: a plant mitochondrial genome annotator. *Plant Communications* **5**: 101191. https://doi.org/10.1016/j.xplc.2024.101191

Liu GH, You-Zuo YW, Shan Y, Yu J, Li JX, Chen Y, Gong XY, Liao XM. 2024. Structural analysis of the mitochon-

drial genome of *Santalum album* reveals a complex branched configuration. *Genomics* **116**: 110935. https://doi.org/10.1016/j.ygeno.2024.110935

McBride HM, Neuspiel M, Wasiak S. 2006. Mitochondria: more than just a powerhouse. *Current Biology* **16**: R551-R560. https://doi.org/10.1016/j.cub.2006.06.054

Molina J, Hazzouri KM, Nickrent D, Geisler M, Meyer RS, Pentony MM, Flowers JM, Pelser P, Barcelona J, Inovejas SA, Uy I, Yuan W, Wilkins O, Michel C-I, LockLear S, Concepcion GP, Purugganan MD. 2014. Possible loss of the chloroplast genome in the parasitic flowering plant *Rafflesia lagascae* (Rafflesiaceae). *Molecular Biology and Evolution* **31**: 793-803. https://doi.org/10.1093/molbev/msu051

Morales-Saldaña S, Barraza-Ochoa AI, Villafán E, Vásquez-Aguilar AA, Ramírez-Barahona S, Ibarra-Laclette E, Ornelas JF. 2025. Comparative plastomes of five *Psittacanthus* species: genome organization, structural features, and patterns of pseudogenization and gene loss. *AoB Plants* **17**: plaf032. https://doi.org/10.1093/aobpla/plaf032

Mower JP. 2020. Variation in protein gene and intron content among land plant mitogenomes. *Mitochondrion* **53**: 203-213. https://doi.org/10.1016/j.mito.2020.06.002

Mower JP, Stefanović S, Young GJ, Palmer JD. 2004. Gene transfer from parasitic to host plants. *Nature* **432**: 165-166. https://doi.org/10.1038/432165b

Mower JP, Stefanović S, Hao W, Gummow JS, Jain K, Ahmed D, Palmer JD. 2010. Horizontal acquisition of multiple mitochondrial genes from a parasitic plant followed by gene conversion with host mitochondrial genes. *BMC Biology* **8**: 150. https://doi.org/10.1186/1741-7007-8-150

Nhat Nam N, Pham Anh Thi N, Khoa Do HD. 2024. New Insights into the diversity of mitochondrial plastid DNA. *Genome Biology and Evolution* **16**: evae184. https://doi.org/10.1093/gbe/evae184

Nickrent DL. 2020. Parasitic angiosperms: how often and how many? *Taxon* **69**: 5-27. https://doi.org/10.1002/tax.12195

Nickrent DL, Anderson F, Kuijt J. 2019. Inflorescence evolution in Santalales: integrating morphological characters and molecular phylogenetics. *American Journal of Botany* **106**: 402-414. https://doi.org/10.1002/ajb2.1250

Notsu Y, Masood S, Nishikawa T, Kubo N, Akiduki G, Nakazono M, Hirai A, Kadowaki K. 2002. The complete sequence of the rice (*Oryza sativa* L.) mitochondrial genome: frequent DNA sequence acquisition and loss during the evolution of flowering plants. *Molecular Genetics and Genomics* **268**: 434-45. https://doi.org/10.1007/s00438-002-0767-1

Ortiz-Rodriguez AE, Guerrero EY, Ornelas JF. 2018. Phylogenetic position of Neotropical *Bursera*-specialist mistletoes: the evolution of deciduousness and succulent leaves in *Psittacanthus* (Loranthaceae). *Botanical Sciences* **96**: 443-461. https://doi.org/10.17129/botsci.1961

Petersen G, Anderson B, Braun H-P, Meyer EH, Møller IM. 2020. Mitochondria in parasitic plants. *Mitochondrion* **52**: 173-182. https://doi.org/10.1016/j.mito.2020.03.008

Petersen G, Cuenca A, Møller IM, Seberg O. 2015 Massive gene loss in mistletoe (*Viscum*, Viscaceae) mitochondria. *Scientific Reports* **5**: 17588. https://doi.org/10.1038/srep17588

Queijeiro-Bolaños ME, Carrillo-Angeles IG, Cervantes-Jiménez M, Suzán-Azpiri H. 2025. Phenology of *Psittacanthus palmeri* (Loranthaceae), a deciduous mistletoe, and its host *Bursera fagaroides*. *Flora* **326**: 152707. https://doi.org/10.1016/j.flora.2025.152707

Schneider AC, Chun H, Stefanović S, Baldwin BG. 2018. Punctuated plastome reduction and host-parasite horizontal gene transfer in the holoparasitic plant genus *Aphyllon*. *Proceedings of the Royal Society B: Biological Sciences* **285**: 20181535. https://doi.org/10.1098/rspb.2018.1535

Skippington E, Barkman TJ, Rice DW, Palmer JD. 2015. Miniaturized mitogenome of the parasitic plant *Viscum scurruloideum* is extremely divergent and dynamic and has lost all nad genes. *Proceedings of the National Academy of Sciences* **112**: E3515-E3524. https://doi.org/10.1073/pnas.1504491112

Skippington E, Barkman TJ, Rice DW, Palmer JD. 2017. Comparative mitogenomics indicates respiratory competence in parasitic *Viscum* despite loss of complex I and extreme sequence divergence, and reveals horizontal gene transfer and remarkable variation in genome size. *BMC Plant Biology* **17**: 49. https://doi.org/10.1186/s12870-017-0992-8

Sloan DB. 2013. One ring to rule them all? Genome sequencing provides new insights into the 'master circle'model of plant mitochondrial DNA structure. *New Phytologist* **200**: 978-985. https://doi.org/10.1111/nph.12395

Sloan DB, Alverson AJ, Chuckalovcak JP, Wu M, McCauley DE, Palmer JD, Taylor DR. 2012. Rapid evolution of enormous, multichromosomal genomes in flowering plant mitochondria with exceptionally high mutation rates. *Plos Biology* **10**: e1001241. https://doi.org/10.1371/journal.pbio.1001241

Sloan DB, Wu Z. 2014. History of plastid DNA insertions reveals weak deletion and AT mutation biases in angiosperm mitochondrial genomes. *Genome Biology and Evolution* **6**: 3210-3221. https://doi.org/10.1093/gbe/evu253

Stamatakis A. 2014. RAxML version 8: a tool for phylogenetic analysis and post-analysis of large phylogenies. *Bioinformatics* **30**: 1312-1313. https://doi.org/10.1093/bioinformatics/btu033

Tang L, Wang T, Hou L, Zhang G, Deng M, Guo X, Ji Y. 2024. Comparative and phylogenetic analyses of Loranthaceae plastomes provide insights into the evolutionary trajectories of plastome degradation in hemiparasitic plants. *BMC Plant Biology* **24**: 406. https://doi.org/10.1186/s12870-024-05094-5

Teixeira-Costa L, Davis CC. 2021. Life history, diversity, and distribution in parasitic flowering plants. *Plant Physiology* **187**: 32-51. https://doi.org/10.1093/plphys/kiab279

Tillich M, Lehwark P, Pellizzer T, Ulbricht-Jones ES, Fischer A, Bock R, Greiner S. 2017. GeSeq –versatile and accurate annotation of organelle genomes. *Nucleic Acids Research* **45**: W6-W11. https://doi.org/10.1093/nar/gkx391

Walker BJ, Abeel T, Shea T, Priest M, Abouelliel A, Sakthikumar S, Cuomo CA, Zeng QD, Wortman J, Young SK, Earl AM. 2014. Pilon: an integrated tool for comprehensive microbial variant detection and genome assembly improvement. *Plos One* **9**: e112963. https://doi.org/10.1371/journal.pone.0112963

Wang D, Rousseau-Gueutin M, Timmis JN. 2012. Plastid sequences contribute to some plant mitochondrial genes. *Molecular Biology and Evolution* **29**: 1707-1711. https://doi.org/10.1093/molbev/mss016

Wang D, Zhang Y, Zhang Z, Zhu J, Yu J. 2010. KaKs_Calculator 2.0: a toolkit incorporating gamma-series methods and sliding window strategies. *Genomics, Proteomics and Bioinformatics* **8**: 77-80. https://doi.org/10.1016/S1672-0229(10)60008-3

Westwood JH, Yoder JI, Timko MP, dePamphilis CW. 2010. The evolution of parasitism in plants. *Trends in Plant Science* **15**: 227-235. https://doi.org/10.1016/j.tplants.2010.01.004

Wicke S, Müller KF, DePamphilis CW, Quandt D, Bellot S, Schneeweiss GM. 2016. Mechanistic model of evolutionary rate variation en route to a nonphotosynthetic lifestyle in plants. *Proceedings of the National Academy of Sciences* **113**: 9045-9050. https://doi.org/10.1073/pnas.1607576113

Wolfe KH, Morden CW, Palmer JD. 1992. Function and evolution of a minimal plastid genome from a nonphotosynthetic parasitic plant. *Proceedings of the National Academy of Sciences* **89**:10648-10652. https://doi.org/10.1073/pnas.89.22.10648

Wynn EL, Christensen AC. 2019. Repeats of unusual size in plant mitochondrial genomes: identification, incidence and evolution. *G3: Genes, Genomes, Genetics* **9**: 549-559. https://doi.org/10.1534/g3.118.200948

Yu R, Sun C, Liu Y, Zhou R. 2021. Shifts from *cis*-to *trans*-splicing of five mitochondrial introns in *Tolypanthus maclurei*. *PeerJ* **9**: e12260. https://doi.org/10.7717/peerj.12260

Yurina NP, Odintsova MS. 2016. Mitochondrial genome structure of photosynthetic eukaryotes. *Biochemistry (Moscow)* **81**: 101-113. https://doi.org/10.1134/S0006297916020048.

Zancani M, Braidot E, Filippi A, Lippe G. 2020. Structural and functional properties of plant mitochondrial F-ATP synthase. *Mitochondrion* **53**: 178-193. https://doi.org/10.1016/j.mito.2020.06.001

Zervas A, Petersen G, Seberg O. 2019. Mitochondrial genome evolution in parasitic plants. *BMC Evolutionary Biology* **19**: 87. https://doi.org/10.1186/s12862-019-1401-8

Zhang X, Chen H, Ni Y, Wu B, Li, J, Burzyński A, Liu C. 2024. Plant mitochondrial genome map (PMGmap): a soft-

ware tool for the comprehensive visualization of coding, noncoding and genome features of plant mitochondrial genomes. *Molecular Ecology Resources* **24**: e13952. https://doi.org/10.1111/1755-0998.13952

Zhang D, Gao F, Jakovlić I, Zou H, Zhang J, Li WX, Wang GT. 2020. PhyloSuite: an integrated and scalable desktop platform for streamlined molecular sequence data management and evolutionary phylogenetics studies. *Molecular Ecology Resources*, **20**: 348-355. https://doi.org/10.1111/1755-0998.13096

Associate editor: Eduardo Ruiz Sánchez

Author Contributions: SMS, conceptualization, developed the original idea, methodology and analyses, writing -original draft preparation, and read and reviewed drafts of the paper and agreed to the published version of the manuscript. JFO, conceptualization, developed the original idea, resources, writing -review and editing, supervision, administration, funding acquisition, and read and reviewed drafts of the paper and agreed to the published version of the manuscript.

Supporting agencies (alphabetical order): This study was supported by two grants from the Consejo Nacional de Ciencia y Tecnología (CONACyT), Mexico, under grant numbers [155686, A1-S-26134] and research funds from the Departamento de Biología Evolutiva, Instituto de Ecología, A.C. (20030/10563) awarded to JFO. SMS is supported by a postdoctoral fellowship (I1200/311/2023) from the Consejo Nacional de Humanidades, Ciencias, y Tecnologías (CONAHCyT) program 'Estancias Posdoctorales por México'. Permission to conduct our fieldwork was granted by the Mexican government (Instituto Nacional de Ecología, Secretaría del Medio Ambiente y Recursos Naturales, SGPA/DGGFS/712/1299/12, SGPA/DGVS/03268/21).

Conflict of interests: The authors declare that there is no conflict of interest, financial or personal, in the information, presentation of data and results of this article.